

DOI: 10.1002/zaac.202400212

The Missing Tb₂O₂NCN Compound: Synthesis, Characterization, and Luminescent Properties

Juan Medina-Jurado, Hicham Bourakhouadar, Alex J. Corkett, David Enseling, Thomas Jüstel, and Richard Dronskowski*

Dedicated to Professor Gordon J. Miller, colleague and friend, on the occasion of his 65th birthday

Advances in the synthetic methods often lead to the discovery of new materials, and nitridocarbonates based on the NCN^{2−} anion are no exception. Recent momentum in preparation processes and improved understanding of the chemistry of these compounds has resulted in many “missing compounds” now being accessible. Accordingly, the synthesis of the terbium oxide carbodiimide Tb₂O₂NCN is reported herein, one of the missing members in the family of rare-earth compounds with the general

formula Ln₂O₂NCN. It is prepared via a solid-state metathesis reaction at 600 °C between TbOCl and Li₂NCN, and its structure is determined from powder X-ray diffraction data to crystallize isotypically to the Ln₂O₂NCN family with Ln = Ce–Yb (except for promethium) in the trigonal $P\bar{3}m1$ space group. The crystal structure is best described as alternating layers of NCN^{2−} anions and Tb₂O₂²⁺ layers along the *c*-axis. Photoluminescence measurements reveal a green emission at room temperature.

1. Introduction

The history of rare-earth oxide carbodiimides, Ln₂O₂NCN, gives a nice example of how preparative methods for such compounds have evolved.^[1–5] It is already 30 years since Hashimoto et al. reported the unexpected synthesis of the first members of this family (Ln = La–Nd, Sm–Gd) by reacting Ln₂O₃ with ammonia in graphite boats at 950 °C, surprisingly leading to graphite-boat corrosion and the aforementioned series of compounds.^[6] A few years later, a second group of compounds was synthesized in China in a more directed 850 °C solid-state reaction between Ln₂O₃ and melamine (C₃H₆N₆). The higher temperature induces the decomposition of melamine and the subsequent formation of the oxide carbodiimide, giving another series with Ln = Dy–Yb.^[7] The astute reader may notice that, excluding the radioactive Pm, the Tb analogue is still missing from this family.

In recent times, solid-state metathesis (SSM) reactions have proved highly effective for synthesizing various rare-earth carbodiimides, providing milder conditions that allow access to thermally labile compounds.^[8,9] In addition, this method assures a certain degree of control as regards the final product via the stoichiometry of the reactants so that the family of phases

incorporating lanthanide Ln³⁺ ions is very diverse, including binary compounds Ln₂(NCN)₃ containing only the carbodiimide unit, or mixed-anion compounds such as Ln₂O(NCN)₂, LnX(NCN), and Ln₂X₂(NCN) with X = F, Cl, not to forget the family of compounds we are dealing with here, Ln₂O₂NCN.^[10–15] Their crystal structure is closely related to their sulfide analogues, Ln₂O₂S, which consists of alternating layers of Ln₂O₂²⁺ and S^{2−} anions.^[16] Then, by replacing the spherical sulfides by the linear NCN unit, extended layered structures are obtained which best reproduce the observed experimental diffraction pattern of Ln₂O₂NCN.^[6,7,17] Over the years, this structural analogy with the chalcogenides has become more pronounced and less surprising. This is to say that the vast field of chalcogenides can be favorably used for a variety of conceptual purposes, such as structure elucidation or as a source of inspiration for the synthesis of new carbodiimide/cyanamide compounds.^[18,19]

Herein, we report the synthesis and photoluminescent properties of the terbium(III) oxide carbodiimide Tb₂O₂NCN prepared by SSM at 600 °C, under much milder conditions than previously used to prepare the rest of the Ln₂O₂NCN family. The crystal structure is the same as that reported for all those phases and, as expected, the lattice parameters and molar volume of Tb₂O₂NCN fit perfectly with the crystallographic data of the previously reported oxide carbodiimides, thus completing the puzzle.

2. Results and Discussion

An SSM between Li₂NCN and TbOCl in a 1:2 ratio was used to prepare terbium(III) oxide carbodiimide according to reaction (1):



The coproduced metathesis salt, LiCl, was removed by washing the air-stable compound with water; subsequent

J. Medina-Jurado, A. J. Corkett, R. Dronskowski
Chair of Solid-State and Quantum Chemistry, Institute of Inorganic Chemistry, RWTH Aachen University, 52056 Aachen, Germany
E-mail: drons@HAL9000.ac.rwth-aachen.de
H. Bourakhouadar, D. Enseling, T. Jüstel
Department of Chemical Engineering, FH Münster University of Applied Sciences, 48565 Steinfurt, Germany

© 2025 The Author(s). Zeitschrift für anorganische und allgemeine Chemie published by Wiley-VCH GmbH. This is an open access article under the terms of the Creative Commons Attribution License, which permits use, distribution and reproduction in any medium, provided the original work is properly cited.

measurements were performed on the washed sample. A powder X-ray diffractogram of the phase-pure material was indexed to a trigonal unit cell with $a = 3.7499 \text{ \AA}$, $c = 8.2024 \text{ \AA}$, giving a volume of $V = 99.89 \text{ \AA}^3$ and reflections consistent with space group $P\bar{3}m1$, suggesting $\text{Tb}_2\text{O}_2\text{NCN}$ to be isostructural with the rest of the $\text{Ln}_2\text{O}_2\text{NCN}$ family with $\text{Ln} = \text{Ce}–\text{Gd}$, $\text{Dy}–\text{Yb}$. A structural model was generated by replacing Ln(III) by terbium(III) at the $2d$ site of $\text{Ln}_2\text{O}_2\text{NCN}$, and then refined using GSAS. A Rietveld fit is presented in **Figure 1**, showing very good agreement between observed and calculated intensities. Crystallographic data are presented in **Table 1** with selected bond lengths and angles in **Table 2**.

Just like the previously reported $\text{Ln}_2\text{O}_2\text{NCN}$ in $P\bar{3}m1$, the crystal structure of $\text{Tb}_2\text{O}_2\text{NCN}$ (**Figure 2**) consists of an alternating sequence of $\text{Tb}_2\text{O}_2^{2+}$ and NCN^{2-} layers along the $[001]$ stacking direction. In the $\text{Tb}_2\text{O}_2^{2+}$ layers, the coordination environment of the terbium cation can be understood as a highly distorted octahedron with space for an extra bond at the axial position (parallel to the stacking direction), so the coordination number is $6 + 1 = 7$: three nitrogen and three “ O_e ” atoms in the equatorial positions are forming an octahedra, and the bond to the “ O_a ” atom in the axial position completes the coordination sphere (Figure 2c). The $\text{Tb}_2\text{O}_2^{2+}$ layers consist of two individual terbium and oxygen sheets in an offset honeycomb arrangement so that the terbium atoms of each sheet are eclipsed by the

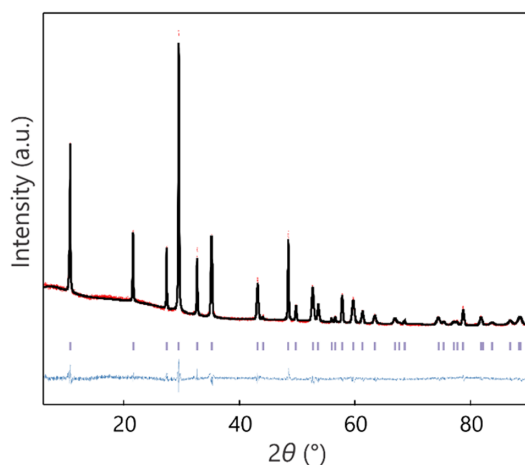


Figure 1. Rietveld fit of $\text{Tb}_2\text{O}_2\text{NCN}$ to PXRD data, showing observed (red), calculated (black), and difference (blue) intensities. Bragg positions of $\text{Tb}_2\text{O}_2\text{NCN}$ (violet) are denoted by vertical markers.

Table 1. Crystallographic data and fractional coordinates for $\text{Tb}_2\text{O}_2\text{NCN}$. Standard deviations are given in parentheses.					
Atom		x	y	z	$U_{\text{iso}} (10^2 \text{ \AA}^2)$
Tb	2d	1/3	2/3	0.1794(1)	1.54(1)
O	2d	0	0	1/2	1.87(8)
N	1b	1/3	2/3	0.8920(8)	2.07(4)
C	2c	0	0	0.3452(2)	"
Trigonal, $P\bar{3}m1$ (no. 164), $Z = 1$, $a = 3.74996(3) \text{ \AA}$, $c = 8.2024(1) \text{ \AA}$; $V = 99.892(2) \text{ \AA}^3$. $R_{\text{wp}} = 3.79\%$, $R_p = 2.96\%$.					

Table 2. Selected bond lengths and angles in $\text{Tb}_2\text{O}_2\text{NCN}$.

Bond lengths (Å)	
Tb–O1	2.358(7)
Tb–O2	2.243(2)
Tb–N	2.557(6)
C–N	1.27(1)
Bond angles (°)	
Tb–O1–Tb	105.1(2)
Tb–O2–Tb	113.4(1)
Tb–N–Tb	94.3(3)
Tb–N–C	122.1(2)
N–C–N	180

oxygen atoms of the next sheet, thus resulting in the equatorial oxygen for the Tb^{3+} in one layer to be the axial oxygen for the Tb^{3+} in the other layer, and *vice versa*. The Tb–O bond lengths are $2.243(2) \text{ \AA}$ for the equatorial bonds (with O_e) and $2.358(7) \text{ \AA}$ for the axial bond (with O_a), and the Tb–N distance at $2.557(6) \text{ \AA}$ resembles the average distances observed in other $\text{Ln}_2\text{O}_2\text{NCN}$ compounds. The molar volume of $\text{Tb}_2\text{O}_2\text{NCN}$ (Tb^{3+} , ionic radius = 0.923 \AA for sixfold coordination) fits perfectly to the analogous compounds with Eu^{3+} (0.947 \AA) and Dy^{3+} (0.912 \AA).^[20] The effect on the volume of the well-known lanthanide contraction for the Tm–Pr series in the $\text{Ln}_2\text{O}_2\text{NCN}$ family is given in **Figure 3**.

A single crystallographically distinct NCN moiety is present in $\text{Tb}_2\text{O}_2\text{NCN}$, which is linear running parallel to the $[001]$ direction with a symmetry-given linear bond angle of $\text{N–C–N} = 180^\circ$. The C–N distance is $1.27(1) \text{ \AA}$, that of a carbon–nitrogen double bond evidencing its carbodiimide character ($\text{N}=\text{C}=\text{N}^-$). This mirrors the expectations since the coordination environment of the NCN unit is highly symmetrical as both terminal nitrogen atoms from each side coordinate similar to three terbium atoms. Further result is provided by infrared (IR) measurements (**Figure 4**) which show the deformation vibration (δ) at 600 cm^{-1} , asymmetric vibrations (ν_{as}) around 2100 cm^{-1} but no symmetric vibration (ν_s) that is only IR-active for the asymmetric cyanamide form ($\text{N}=\text{C}=\text{N}^{2-}$).

To investigate the photoluminescent properties of single-phase $\text{Tb}_2\text{O}_2\text{NCN}$, excitation and emission spectra were recorded at room temperature, as shown in **Figure 5**. By monitoring the emission at 543 nm , the excitation spectrum shows a relatively broadband ($\text{FWHM} = 5500 \text{ cm}^{-1}$) between 220 and 320 nm , with a maximum at 270 nm . Moreover, weaker absorption line multiplets are revealed between 315 and 390 nm , which can be assigned to the intraconfigurational transitions 7F_6 to 5D_3 , 5G_3 , and 5H_7 of Tb^{3+} . Upon excitation at 270 nm at room temperature, $\text{Tb}_2\text{O}_2\text{NCN}$ exhibits green luminescence. The emission spectrum yields narrow multiplets of emission lines at 487 , 495 , 543 (main emission), 550 and 586 nm , which are attributed to the intraconfigurational $4f–4f$ transitions of Tb^{3+} , i.e., from the lowest excited state 5D_4 to the ground state 7F_J ($J = 6, 5$ and 4) of the $[\text{Xe}]4f^8$ configuration. These results are consistent with those observed for doped (substituted) compounds such as $\text{LiIn}(\text{NCN})_2:\text{Tb}^{3+}$ and $\text{Gd}_2(\text{NCN})_3:\text{Tb}^{3+}$, although in our case we are dealing with a stoichiometric Tb(III) material.^[21,22]

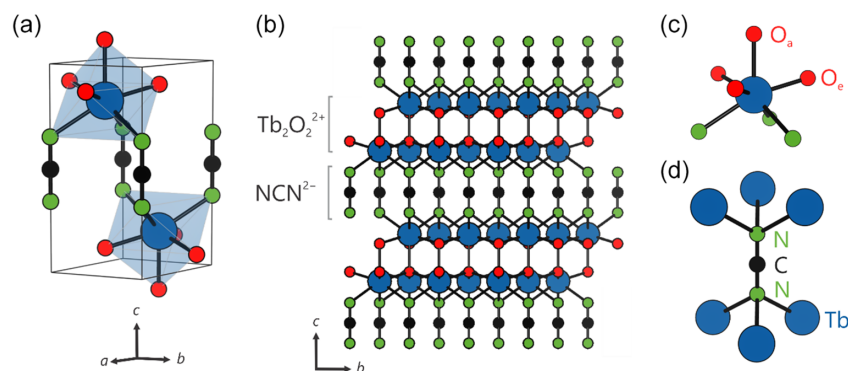


Figure 2. a) Crystal structure of $\text{Tb}_2\text{O}_2\text{NCN}$ in $P\bar{3}m1$. b) Alternating stacking sequence of NCN^{2-} layers with $\text{Tb}_2\text{O}_2^{2+}$ layers. Coordination environment of c) Tb^{3+} and d) the NCN^{2-} unit.

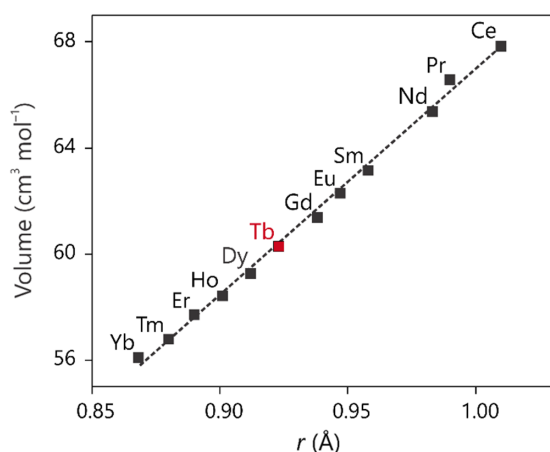


Figure 3. Linear trend (dotted line) for the molar volume against the Ln^{3+} ionic radii of the $\text{Ln}_2\text{O}_2\text{NCN}$ family members including the new $\text{Tb}_2\text{O}_2\text{NCN}$ (in red).

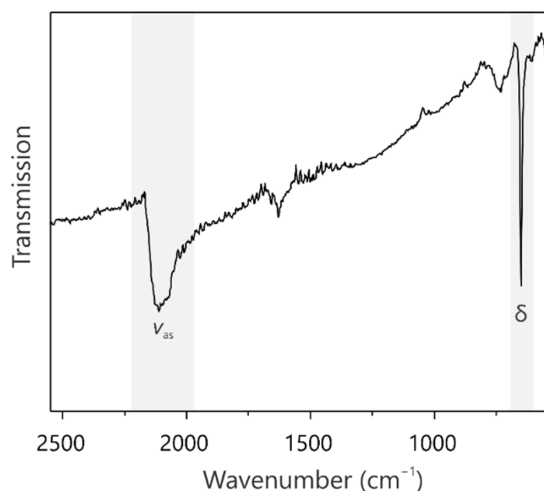


Figure 4. IR spectrum of $\text{Tb}_2\text{O}_2\text{NCN}$. The regions for deformation (δ) and asymmetric vibrations (ν_{as}) are highlighted in gray. We attribute the presence of small vibrational bands around 750 and 1600 cm^{-1} to the presence of a carbonate phase undetected by X-ray diffraction.

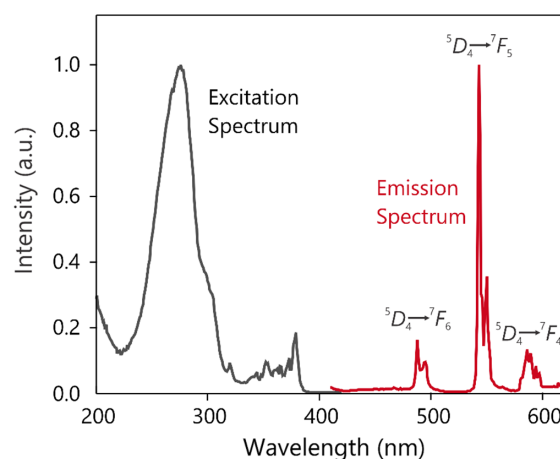


Figure 5. Excitation spectrum of $\text{Tb}_2\text{O}_2\text{NCN}$ at room temperature for 543 nm monitoring emission spectrum upon 270 nm excitation.

3. Conclusions

A metathetic approach allowed to prepare the missing lanthanide oxide carbodiimide $\text{Tb}_2\text{O}_2\text{NCN}$ by a solid-state reaction between Li_2NCN and TbOCl . $\text{Tb}_2\text{O}_2\text{NCN}$ was found to crystallize isostructurally to previously reported $\text{Ln}_2\text{O}_2\text{NCN}$ with $P\bar{3}m1$ symmetry. The carbodiimide character of the NCN unit was confirmed by IR measurements. The crystal structure is best described as a stacking arrangement of $\text{Tb}_2\text{O}_2^{2+}$ sheets alternating with NCN^{2-} layers. Photoluminescence studies reveal that under 270 nm excitation $\text{Tb}_2\text{O}_2\text{NCN}$ emits radiation in the green range, consisting of multiple emission lines with a maximum centered at 543 nm, similar to the pattern exhibited by NCN compounds incorporating Tb^{3+} ions.

4. Experimental Section

Synthesis: $\text{Tb}_2\text{O}_2\text{NCN}$ was synthesized on a 0.5 g scale in an argon-filled glove box by SSM reaction between TbOCl and Li_2NCN with a 2:1 molar ratio. Li_2NCN was prepared under protective atmosphere from Li_3N and melamine ($\text{C}_3\text{N}_6\text{H}_6$) as described in ref. [23]. TbOCl was obtained from slow dehydration of $\text{TbCl}_3 \cdot 6\text{H}_2\text{O}$.^[24]

After homogenization using a mortar and pestle agate, the reaction mixture was placed inside an open dry glass capillary and loaded into a tubular furnace under flowing argon at 600 °C for 18 h, using a heating and cooling rate of 2 °C min⁻¹. The product is an air-stable white-beige powder, which was washed with water and acetone to remove the LiCl metathesis salt, eventually dried at 100 °C.

Powder X-Ray Diffraction Analysis: Powder X-ray diffraction (PXRD) data were recorded on washed Tb₂O₂NCN at room temperature using a calibrated STOE STADI-P powder diffractometer with a flat sample holder (Cu K_{α1}, linear PSD, 2θ range 3–90° with individual steps of 0.005°). Rietveld refinements were performed using GSAS with the EXPGUI interface.^[25] The thermal displacement parameters U_{iso} of C and N were constrained to be equal. Full details concerning the structure determination including all intensity data are available in CIF format and have been deposited under the CCDC entry number 2404642.

IR Measurements: The IR spectra were measured directly from powder on a Shimadzu IRSpirit FT-IR spectrometer in the range 400–4000 cm⁻¹.

Photoluminescence Spectroscopy: A fluorescence spectrometer FLS920 (Edinburgh Instruments) equipped with a 450 W xenon discharge lamp (OSRAM) was employed to record the emission spectra. Into the sample chamber, a mirror optic designed for powder samples was mounted. For detection, an R2658P single-photon-counting photomultiplier tube (Hamamatsu) was utilized.

Acknowledgements

J.M.-J. and H.B. contributed equally to this work. The authors thank Mr T. Storp for his assistance with PXRD measurements. J.M.-J. is grateful for the financial support from Deutscher Akademischer Austauschdienst (DAAD). A.J.C. is indebted to the Deutsche Forschungsgemeinschaft (DFG) for funding (project no. 441856704).

Open Access funding enabled and organized by Projekt DEAL.

Conflict of Interest

The authors declare no conflict of interest.

Data Availability Statement

The data that support the findings of this study are available from the corresponding author upon reasonable request.

Keywords: carbodiimides · luminescence · rare-earths · synthesis · X-ray diffraction

- [1] A. J. Corkett, O. Reckeweg, R. Pöttgen, R. Dronskowski, *Chem. Mater.* **2024**, *36*, 9107.
- [2] O. Sumioka, N. Tarutani, K. Katagiri, K. Inumaru, Z. Lang Goo, K. Sugimoto, Y. Asai, M. Saito, T. Motohashi, *Inorg. Chem.* **2024**, *63*, 15539.
- [3] X. Liu, M. A. Wankeu, H. Lueken, R. Dronskowski, *Z. Naturforsch. B* **2005**, *60*, 593.
- [4] X. Liu, L. Stork, M. Speldrich, H. Lueken, R. Dronskowski, *Chem. Eur. J.* **2009**, *15*, 1558.
- [5] X. Liu, M. Krott, P. Müller, C. Hu, H. Lueken, R. Dronskowski, *Inorg. Chem.* **2005**, *44*, 3001.
- [6] Y. Hashimoto, M. Takahashi, S. Kikkawa, F. Kanamaru, *J. Solid State Chem.* **1996**, *125*, 37.
- [7] M. Li, W. Yuan, J. Wang, C. Gu, *Powder Diffraction* **2007**, *22*, 59.
- [8] H.-J. Meyer, *Dalton Trans.* **2010**, *39*, 5973.
- [9] K. Gibson, M. Ströbele, B. Blaschkowski, J. Glaser, M. Weisser, R. Srinivasan, H. J. Kolb, H.-J. Meyer, *Z. Anorg. Allg. Chem.* **2003**, *629*, 1863.
- [10] M. Neukirch, S. Tragl, H.-J. Meyer, *Inorg. Chem.* **2006**, *45*, 8188.
- [11] R. Srinivasan, S. Tragl, H.-J. Meyer, *Z. Anorg. Allg. Chem.* **2005**, *631*, 719.
- [12] R. Srinivasan, J. Glaser, S. Tragl, H.-J. Meyer, *Z. Anorg. Allg. Chem.* **2005**, *631*, 479.
- [13] L. Unverfehrt, M. Ströbele, J. Glaser, H.-J. Meyer, *Z. Anorg. Allg. Chem.* **2009**, *635*, 1947.
- [14] W. Liao, U. Englert, R. Dronskowski, *Eur. J. Inorg. Chem.* **2006**, *2006*, 4233.
- [15] W. Liao, R. Dronskowski, *Z. Anorg. Allg. Chem.* **2005**, *631*, 496.
- [16] H. A. Eick, *J. Am. Chem. Soc.* **1958**, *80*, 43.
- [17] E. Ionescu, W. Li, L. Wiehl, G. Mera, R. Riedel, *Z. Anorg. Allg. Chem.* **2017**, *643*, 1681.
- [18] P. Kallenbach, M. Ströbele, H.-J. Meyer, *Z. Anorg. Allg. Chem.* **2020**, *646*, 1281.
- [19] K. B. Sterri, C. Besson, A. Houben, P. Jacobs, M. Hoelzel, R. Dronskowski, *New J. Chem.* **2016**, *40*, 10512.
- [20] R. Shannon, *Acta Crystallogr. Sect. A* **1976**, *32*, 751.
- [21] M. Kubus, R. Heinicke, M. Ströbele, D. Ensling, T. Jüstel, H.-J. Meyer, *Mater. Res. Bull.* **2015**, *62*, 37.
- [22] J. Glaser, L. Unverfehrt, H. Bettentrup, G. Heymann, H. Huppertz, T. Jüstel, H.-J. Meyer, *Inorg. Chem.* **2008**, *47*, 1045.
- [23] A. O. Corral, M. Kubus, M. Ströbele, H.-J. Meyer, *Z. Anorg. Allg. Chem.* **2014**, *640*, 902.
- [24] S. Chong, B. Riley, Z. Nelson, *Acta Crystallogr. Sect. E* **2020**, *76*, 621.
- [25] B. H. J. Toby, *Appl. Crystallogr.* **2001**, *34*, 210.

Manuscript received: November 22, 2024

Revised manuscript received: January 24, 2025

Version of record online: March 16, 2025